PHYSICAL REVIEW B **80**, 060403(R) (2009)

Fully relativistic *ab initio* description of spin-polarized STM experiments in terms of magnetic-field-dependent tunneling currents

P. Weinberger
Center for Computational Nanoscience, Seilerstätte 10/22, A-1010 Vienna, Austria
and Max-Planck-Institut für Mikrostrukturphysik, Weinberg 2, Halle, D06120 Saale, Germany
(Received 6 July 2009; revised manuscript received 6 August 2009; published 28 August 2009)

An approach is introduced to interpret spin-polarized scanning tunnel microscope experiments in terms of differences in the tunneling conductivity with respect to different magnetic configurations and the corresponding band energy contribution to the magnetic anisotropy energy, the former being considered to be proportional to the applied external magnetic field. This approach is illustrated for Cu(111) coated with two monolayers of Co considering two types of Cr/W tips. It is found that the reorientation transition of the magnetization in the Co layers can unambiguously be identified even in cases when the tip contributes considerably to the tunneling current difference.

DOI: 10.1103/PhysRevB.80.060403 PACS number(s): 75.70.−i, 68.37.Ef, 75.47.−m, 75.75.+a

Based on Bardeen's suggestion[1] scanning tunnel microscope (STM) experiments are usually interpreted in terms of the so-called Tersoff-Hamann approach[2] in which the tunneling current is replaced by the charge density corresponding to the surface local density of states. Frequently also attempts are made to include approximations for Bardeen's matrix element, which, however, in its original form is very difficult to evaluate since it combines nonorthogonal eigenstates of different Hamiltonians, namely, those "of the probe" and "of the surface." Mostly these approximations are based on spherically shaped tips[2] and using an *s*-wave for the tip wave function. The use of the Tersoff-Hamann approach turned out to be extremely successful in interpreting experimental structural data.[3] With the arrival of spin-polarized STM techniques, however, different theoretical approaches capable of describing not only noncollinear spin structures but also the magnetic properties of the tip are required. Although the usual Tersoff-Hamann approach can be extended to a spin-polarized *ab initio* level, the difficulties with Bardeen's matrix elements remain and, in particular, one of the main features of these techniques, namely, including an external magnetic field, cannot be described properly.

A spin-polarized STM equipment suitable to describe the reorientation transition of Co nanostructures on a Cu substrate—probably the experimentally best studied system—is modeled in here by a layered structure, namely, $\mathrm{Cu}(111)/\mathrm{Cu}_m\mathrm{Co}_2\mathrm{Vac}_3\mathrm{Cr}_n\mathrm{W}_p\mathrm{Cu}_q/\mathrm{Cu}$-lead, where m and q refer to the number of Cu layers needed to join up smoothly to either the semi-finite substrate or the semi-infinite Cu lead; n denotes the number of Cr layers and p those of W. It is important to note that in order to pass a current through the system on the sample side the substrate plays the role of a lead, while on the tip side the W slab is connected to a Cu lead. Therefore, both, the substrate as well as the Cu lead serve as electron reservoirs. The directions of the current and the external magnetic field are assumed in accordance with most experiments to be parallel or antiparallel to the surface normal.

Since in principle each atomic layer characterized by two-dimensional translational symmetry can have a different orientation of the magnetization,[4] this multitude of possibilities is reduced to a few cases such as rotating the orientation of the magnetization in the subsystems $[\mathrm{Cu}_m\mathrm{Co}_2\mathrm{Vac}_1]$ ("sample") and $[\mathrm{Vac}_1\mathrm{Cr}_n\mathrm{W}_p\mathrm{Cu}_q]$ ("tip") separately by say ϕ_1 and ϕ_2, where the ϕ are rotation angles around the (in plane) $\hat{y}$ axis. Since even then all quantities such as, e.g., the anisotropy energy would form surfaces in the (ϕ_1, ϕ_2) space, only the cases listed in Table I were considered. In this table configuration C_0 corresponds to a reference state, in which the orientation of the magnetization points uniformly along the surface normal; configuration C_5 refers to a uniform rotation by ϕ_1.

All *ab initio* calculations were performed at the experimental lattice constant of Cu in terms of the spin-polarized (fully) relativistic screened Korringa-Kohn-Rostoker (SPR-KKR) method.[5] The electric transport properties were evaluated by means of the fully relativistic Kubo-Greenwood equation.[4] In order to reduce the computational effort for the

TABLE I. Magnetic configurations considered, $0 \leq \phi_1 \leq 2\pi$, $0 \leq \phi_2 \leq \pi$.

Config.	$[\mathrm{Cu}_m\mathrm{Co}_2]$	Vac_1	Vac_2	Vac_3	$[\mathrm{Cr}_n\mathrm{W}_p\mathrm{Cu}_q]$
C_0	0	0	0	0	0
C_1	ϕ_1	ϕ_1	0	0	0
C_2	0	0	0	ϕ_1	ϕ_1
C_3	0	ϕ_1	ϕ_1	ϕ_1	ϕ_1
C_4	90	90	ϕ_2	ϕ_2	ϕ_2
C_5	ϕ_1	ϕ_1	ϕ_1	ϕ_1	ϕ_1

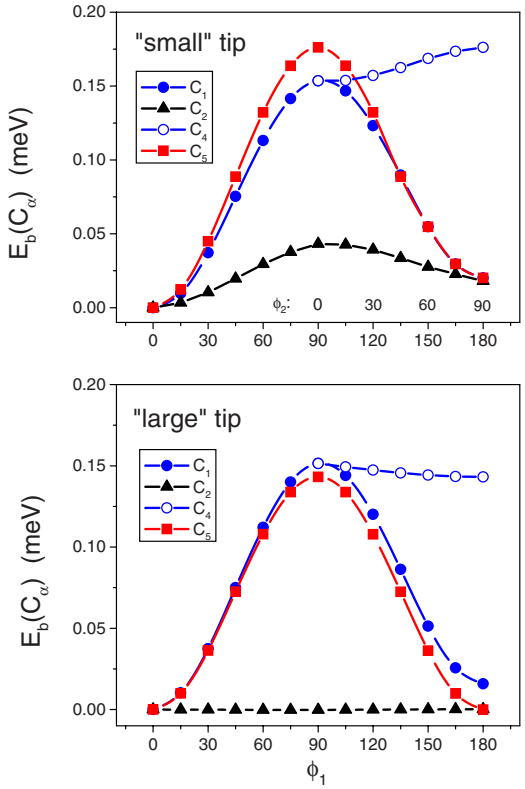

FIG. 1. (Color online) Band energy part of the anisotropy energy $E_b(C_\alpha)$, see also Table I. For convenience ϕ_2 is marked separately.

anisotropy and conductivity calculations $m=q=15$ were chosen with two different tips, namely, $n=3$, $p=7$ ("small" tip) and $n=15$, $p=22$ ("large" tip). As the interlayer distance in Cu(111) is 2.087 Å, the vacuum barrier is about 6 Å wide.

In principle the magnetic anisotropy energy $E_a(C_\alpha)$ consists of two parts,[4,5] the so-called band energy contribution $E_b(C_\alpha)$ and the magnetic dipole-dipole interaction energy $E_{dd}(C_\alpha)$. In the present context only the band energy part, i.e., the free energy at zero temperature, will be considered since this energy is considered to be proportional to the applied external field,

$$E_b(C_\alpha) = E(C_\alpha) - E(C_0), \tag{1}$$

where $E(C_\alpha)$ is the band energy[4,5] for a particular configuration.

In Fig. 1 the band energies $E_b(C_\alpha)$ are displayed for most of the configurations listed in Table I. As can be seen when varying the orientation of the magnetization uniformly, the corresponding band energy $E_b(C_5)$ follows closely that when changing the direction of the magnetization only in the sample part, $E_b(C_1)$. Decoupling the orientation of the magnetization in the vacuum layers (configuration C_3, "surface state") from that in the top Co layer results in a band energy of the form $0.435(1-\cos\phi_1)$ (meV) and is therefore unlikely to be seen experimentally. It is worthwhile to mention that the values of $E_b(C_1)$ at 90° are very close to that reported[6] for a free surface of Cu(111) coated with two monolayers of Co. In this reference also the corresponding magnetic dipole-dipole energy $E_{dd}(C_1)$ and the effects of relaxation are discussed.

The local current in layer i for a particular magnetic configuration in the presence of all other currents, $j_z^i(C_\alpha)$, is defined by[4,5]

$$j_z^i(C_\alpha) = L^{-1}\sum_j \sigma_{zz}^{ij}[(C_\alpha\ ]E_z^j, \tag{2}$$

where the $\sigma_{zz}^{ij}(C_\alpha)$ are the (layerwise) matrix elements of the zz-like conductivity tensor, L is the total number of atomic layers considered (72 in the case of the large tip), and E_z^j is the electric field in layer j, considered in the following to be uniform in all layers. The total current is then given by the sum over all layers i. It should be noted that per definition the local currents $j_z^i(C_\alpha)$ need not to be positive for all i, only the total current has to fulfill this property.

The local and total difference between a particular magnetic configuration and the reference configuration C_0 can be simply defined as

$$\Delta j_z(C_\alpha) = E_z\sum_i \Delta\sigma_{zz}^i(C_\alpha), \tag{3}$$

$$\Delta\sigma_{zz}^j(C_\alpha) = L^{-1}\sum_j [\sigma_{zz}^{ij}(C_0) - \sigma_{zz}^{ij}(C_\alpha)]. \tag{4}$$

From Fig. 2 it can be seen that for both types of tips $\Delta j_z^i(C_1)$ has a sharp peak when i refers to the top Co layer. This peak grows as ϕ_1 approaches 90°, i.e., approaches an in-plane orientation of the magnetization in the Co layers. Since this is the by far largest contribution to the total difference current $\Delta j_z(C_1)$, see Eq. (4), Fig. 2 proves that in principle a spin-polarized STM experiment can be (almost) atom specific, provided, however, that changes in the orientation of the magnetization in the tip part of the system do not alter this finding. Such a situation can already be gathered from the $\Delta j_z^i(C_2)$ entries in Fig. 2 in the case of the small tip. It turned out that in this case the contributions to $\Delta j_z(C_2)$ arising from the Cr and the W layer forming the Cr/W interface, see Fig. 2, are the largest ones.

With the exception of C_4 all other investigated total current differences $\Delta j_z(C_\alpha)$, see Fig. 3, have a maximum at 90°, whereby as to be expected from Fig. 2 the values corresponding to C_1 and C_5 in the case of the large tip are nearly the same. It should be noted in particular that if for a specific configuration $E_b(C_\alpha)\sim 0, \forall\phi$, then also $\Delta\sigma_{zz}(C_\alpha)\sim 0, \forall\phi$, see configuration C_2 in Figs. 2 and 3 in the case of the large tip, i.e., it is indeed important to use a relativistic description for both, the band energy and the conductivity.

Clearly enough, by considering only the current as a function of the orientation of the magnetization in the two subsystems this does not give a clear view of what is actually recorded in a spin-polarized STM experiment. In order to answer this question one has to remember that in such an experiment a current difference is measured as a function of an external magnetic field. Since the band energy is proportional to the applied magnetic field the theoretically calculated current difference ought to be viewed as an implicit function of the band energy. Put in words this means that for

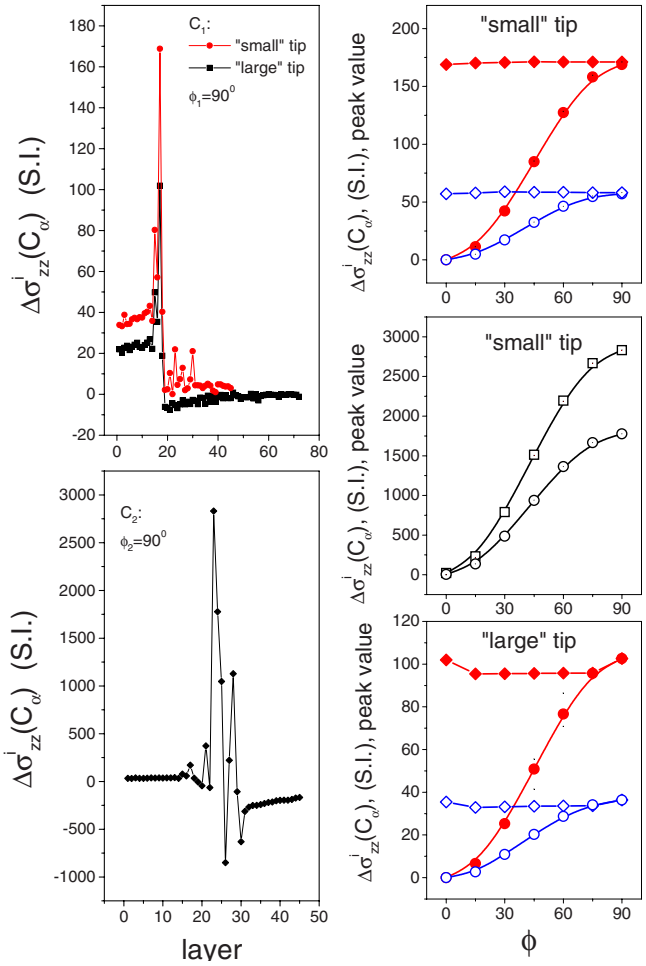

FIG. 2. (Color online) Layer-resolved difference conductivities $\Delta\sigma^i_{zz}(C_\alpha)$, see Eq. (3) and Table I. Left column: $\Delta\sigma^i_{zz}(C_1)$ for both types of tips (top) and $\Delta\sigma^i_{zz}(C_2)$ (bottom). Right column: peak values of $\Delta\sigma^i_{zz}(C_1)$ (circles) and $\Delta\sigma^i_{zz}(C_4)$ (diamonds) corresponding to the top Co layer (full symbols) and the Co layer below (open symbols) for the small tip (top) and the large tip (bottom). For the Cr (open squares) and W (open circles) layers forming the Cr/W interface the peak values of $\Delta\sigma^i_{zz}(C_2)$ are displayed in the middle entry of the right column in the case of the small tip.

a given value of ϕ in a particular configuration C_α the respective difference conductivity $\Delta\sigma^i_{zz}(C_\alpha)$ is to be displayed versus the corresponding anisotropy energy $E_b(C_\alpha)$, i.e.,

$$\Delta j_z(E_b) = E_z \sum_i \Delta\sigma^i_{zz}(E_b). \tag{5}$$

Considering current differences as a function of the (lowest ascending) band energy, one finally arrives at a decisive description of the contrast to be seen in experiments. As the reference configuration C_0 listed in Table I is only a matter of convention, in Fig. 4 for matters of convenience the band energy is shifted with respect to configuration $C_1, \phi_1 = 90$, i.e., is given in terms of $H = E_b - E_b(C_1, \phi_1 = 90)$, since experimentally at zero field (ground state) an in-plane orientation of the magnetization in the Co layers applies. From Fig. 4 follows, e.g., that in the case of the small tip for $H \leq 0$ only changes in the Co-related part are recorded, while for bigger

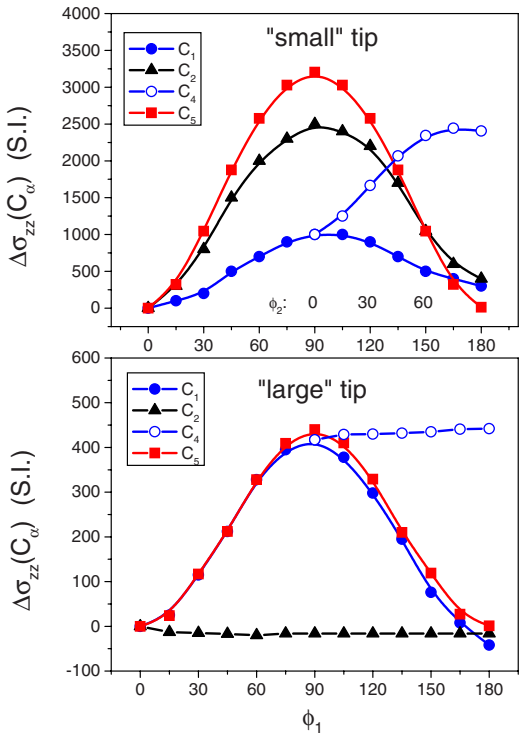

FIG. 3. (Color online) Top: difference conductivities $\Delta\sigma_{zz}(C_\alpha)$, see Eq. (4) and Table I. For convenience ϕ_2 is also marked.

values of H also the signature of the tip shows up. Quite obviously having the reorientation transition of the magnetization in the Co layers in mind, this transition can be picked up experimentally without any doubt, in particular, since Fig. 2 showed that for $H \leq 0$ the main contribution to $\Delta j_z(H)$ arises from the top Co layer. It should be noted that at large enough H a sudden drop in $\Delta j_z(H)$ is visible in Fig. 4. It is caused by $\Delta j_z(C_4)$ when in Fig. 3 ϕ_2, see also Table I, approaches 90°. For $H \leq 0$ the agreement is very good indeed, see the experimental and theoretical values in the encircled area in the case of the small tip, while for $H > 0$, i.e., in the regime, in which the difference conductivity is governed by anisotropy effects from the tip, the increase in band energy obviously is too small.

As in here a model of a spin-polarized STM experiment in terms of a layered system is used, this implies *inter alia* that when moving the tip laterally over the surface a regular array of $\Delta j_z(E_b)$ "signals" has to be picked up, namely, one arising (mostly) from each atom in Co top layer.

Quite clearly the actual structure of a tip is quite a bit more complicated than the simple model used in here. Since very little is known about this structure (thickness of the Cr coating, geometrical shape of the tip, thickness of the W slab, relaxation effects with respect to the Cu lead, or between Cr and W, etc.) only the main effects and the role of each individual part can be pointed out. In Fig. 5 the Madelung potentials for the systems with the small and the large tip are displayed. As can be seen, because of the Cu lead the W level of reference is quite a bit lower than that of Cu. The Madelung potential for the Cr layer forming the surface of the tip, however, is elevated in both cases. It is useful to recall that a surprisingly high value of the surface Madelung

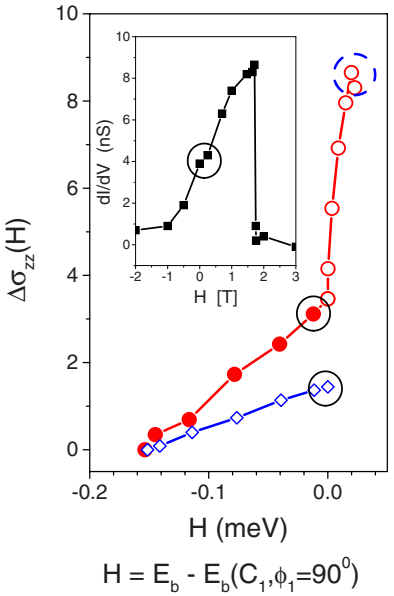

FIG. 4. (Color online) Difference conductivity for the small and the large tip as a function of the band energy. The inset shows the experimental data for Co islands on Cu(111) (Ref. 7). In order to facilitate a direct comparison with the experimental data the band energy is shown with respect to configuration C_1, $\phi_1=90°$ (ground state), the theoretical difference conductivities are scaled linearly such that the value of the peak matches that in the experimental data. The full circle marks the situation when the orientation of magnetization in the Co layers is in plane, the dashed circle when it becomes in plane also in the tip.

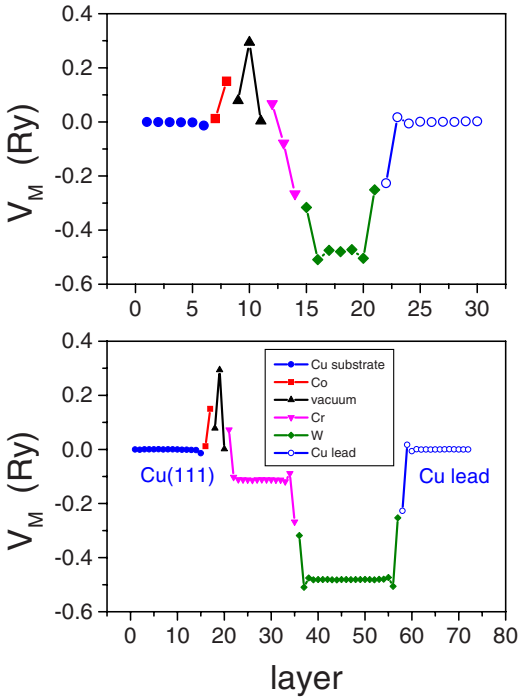

FIG. 5. (Color online) Madelung potentials in the system $Cu(111)/Cu_{15}Co_2Vac_3Cr_nW_pCu_{15}/Cu$ lead. Top: $n=3$ and $p=7$, bottom: $n=15$ and $p=22$. Note that the various atomic species are specified by different symbols.

potential is the actual cause for bcc-Cr(111) or bcc-Cr(100) surfaces to be magnetic although bulk bcc-Cr is nonmagnetic. Figure 5 illustrates the importance of the tip structure close to the vacuum barrier. Furthermore, from this figure the large positive peak caused by the vacuum barrier can be seen. By increasing the width of the vacuum barrier the Madelung potential in the interior of the barrier assumes (about) the same value as that of the corresponding peak in Fig. 5. This is the very reason of why by moving the tip up and down the conductance (resistance) varies rapidly.

Finally, it should be mentioned that by using the so-called embedded cluster method[5,8] and a real space version of the Kubo-Greenwood equation[4,9] not only different shapes of the tip can be accounted for but also difference currents for individual atoms in a cluster of magnetic atoms on top of a nonmagnetic substrate can be investigated. Using this particular combination of methods and the scheme presented in here, in accordance with experimental evidence even a decisive distinction between rim and interior atoms in an island can be established because they possess different anisotropy energies.[10]

I am grateful to J. Kirschner and D. Sander, Max-Planck-Institut für Mikrostrukturphysik in Halle (Germany), for many useful discussions concerning the experimental details.

[1] J. Bardeen, Phys. Rev. Lett. **6**, 57 (1961).
[2] J. Tersoff and D. R. Hamann, Phys. Rev. Lett. **50**, 1998 (1983); Phys. Rev. B **31**, 805 (1985).
[3] D. Drakova, Rep. Prog. Phys. **64**, 205 (2001); J. M. Blanco, F. Flores, and R. Pérez, Prog. Surf. Sci. **81**, 403 (2006).
[4] P. Weinberger, *Magnetic Anisotropies in Nanostructured Matter* (CRC, Boca Raton, FL, 2008).
[5] J. Zabloudil, R. Hammerling, L. Szunyogh, and P. Weinberger, *Electron Scattering in Solid Matter* (Springer, Berlin, 2004).
[6] R. Hammerling, C. Uiberacker, J. Zabloudil, P. Weinberger, L. Szunyogh, and J. Kirschner, Phys. Rev. B **66**, 052402 (2002).
[7] G. Rodary, S. Wedekind, D. Sander, and J. Kirschner, Jpn. J. Appl. Phys. **47**, 9013 (2008); M. Czerner, G. Rodary, S. Wedekind, D. Fedorov, D. Sander, I. Mertig, and J. Kirschner, J. Magn. Magn. Mater. (to be published). In there also a model for antiferromagnetically ordered Cr layers is discussed using a Landauer-type formulation for the tunneling current.
[8] B. Lazarovits, L. Szunyogh, and P. Weinberger, Phys. Rev. B **65**, 104441 (2002).
[9] K. Palotas, B. Lazarovits, L. Szunyogh, and P. Weinberger, Phys. Rev. B **70**, 134421 (2004).
[10] C. Etz, B. Lazarovits, J. Zabloudil, R. Hammerling, B. Újfalussy, L. Szunyogh, G. M. Stocks, and P. Weinberger, Phys. Rev. B **75**, 245432 (2007).